

Polystyrene Nanometer-Sized Particles Supported Alkaline Imidazolium Ionic Liquids as Reusable and Efficient Catalysts for the Knoevenagel Condensation in Aqueous Phase

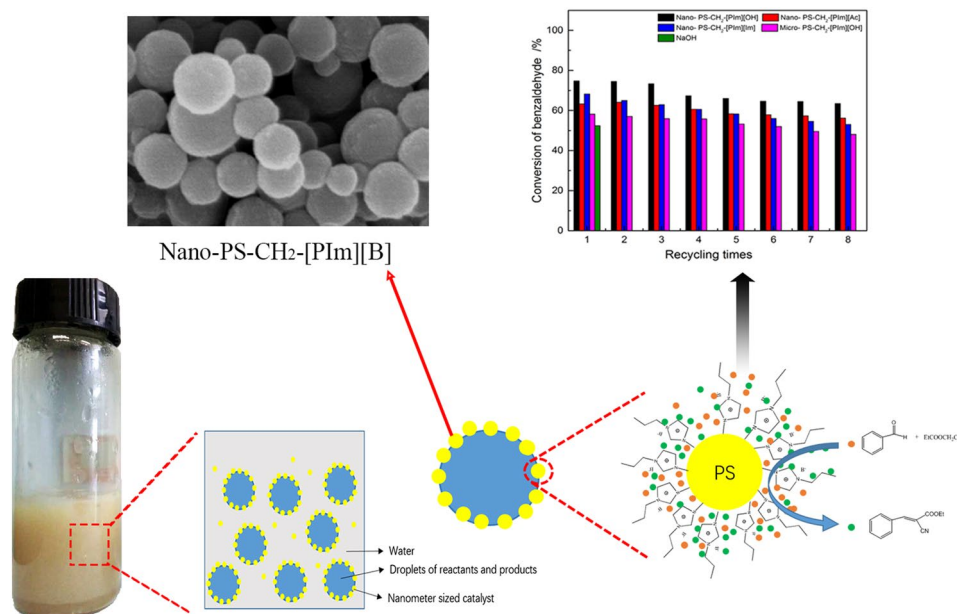
Min Ma¹ · Hansheng Li¹  · Wang Yang¹ · Qin Wu¹ · Daxin Shi¹ · Yun Zhao¹ · Caihong Feng¹ · Qingze Jiao^{1,2}

Received: 7 September 2017 / Accepted: 17 November 2017
© Springer Science+Business Media, LLC, part of Springer Nature 2017

Abstract

Polystyrene nanometer-sized particles supported alkaline 1-propyl imidazolium ionic liquids catalysts (nano-PS-CH₂-[pIM][B]) were prepared and characterized by FT-IR, SEM, TG/DTA, BET and particle size distribution analysis. The results suggested that ionic liquids were successfully loaded on the surface of polymer carriers by covalent bond with high alkali amount. It showed excellent catalytic activities for Knoevenagel condensation especially in aqueous phase, which much higher than that of NaOH and micro-PS-CH₂-[pIM][B]. It will be expected for the potential application of organic reactions in aqueous phase.

Graphical Abstract



Keywords Nanometer size · Supported ionic liquids · Knoevenagel condensation · Aqueous phase

1 Introduction

Ionic liquids (ILs) have increasingly attracted interest as being green solvents and catalysts over the last few decades, mainly due to their excellent properties such as negligible

✉ Hansheng Li
hanshengli@bit.edu.cn

Extended author information available on the last page of the article

vapor pressure, high thermal stability and high reaction activity [1]. In the field of catalysis, ILs can be designed into various structures, which present more opportunities to design and optimize reaction systems [2, 3]. It has been proved that ILs not only enhance the reaction rate to a great extent in many reactions, such as alkylation [4], hydrogenation [5], carbonylation [6], polymerization [7], and enzyme catalysis [8], but also improve the selectivity of the objective products. However, similar to other homogeneous catalysts, ILs are still hampered by several practical drawbacks, namely, catalyst recovery and product purification. Thus, supported ionic liquids (SILs) have been generated to overcome problems mentioned above [9]. It is SILs that ILs covalent on the solid supports like molecular sieves [10], mesoporous silica gels [11], polymers [12, 13], carbon materials [14, 15] and magnetic materials [16], etc. SILs have been extensively evaluated for their attractive features that combine the benefits of ILs with advantages of heterogeneous carriers for designability, ease of handling, separation and recycling [17]. Furthermore, it is desirable to minimize the amount of the utilized ionic liquid in a potential process [18].

Particularly, polymer supported ionic liquids (PSILs) are a series of attractive catalysts for their corrosion resistance to acid and alkali, excellent stability and modifiability [19]. At present, PSILs in the catalytic field are mainly concentrated in two aspects. One is PSILs modified with acidic groups, and applied for a variety of organic reactions as acidic catalysts [20–23]. The other is ILs with transition metal catalyst immobilized on polymer supports to improve the catalytic efficiency and ameliorate stability of metal catalysts [24–30]. The previous reports have shown that polystyrene resin supported acidic ionic liquid catalysts are potential candidates for catalyzing organic reactions like CO₂ cycloaddition reaction [31], Henry reaction [32], acetalization reaction [33] and Fischer esterification [34], etc. Nevertheless, most of their polymer carriers are designed to be amorphous, massive or micrometer-sized particles for easy recycling, but their catalytic performances need to be further enhanced. Provided the recovery of the catalysts, it is foreseeable that the PSILs with nanometer-sized polymer carrier are more likely to express excellent catalytic properties due to their higher specific surface area, more active sites and better dispersion.

The present work described in detail the preparation and catalytic performances of polystyrene nanometer-sized particles supported alkaline 1-propyl imidazole ionic liquids (nano-PS-CH₂-[pIM][B]). The cross-linked chloromethyl functionalized polystyrene nanometer-sized particles (PS-CH₂Cl NPs) were prepared by miniemulsion polymerization. During the synthesis of PSILs, OH⁻, Ac⁻ and Im⁻ as basic anions were introduced by ion exchange separately. These three types of basic catalysts were applied

to catalyze the Knoevenagel condensation of benzaldehyde and ethyl cyanoacetate. Furthermore, polystyrene micrometer-sized particles supported alkaline 1-propyl imidazolium ionic liquids (micro-PS-CH₂-[pIM][B]) was prepared by suspension polymerization in comparison with nano-PS-CH₂-[pIM][B] we concerned about. Attention was concentrated on the catalytic activities of these catalysts for Knoevenagel condensation in aqueous phase.

2 Experimental

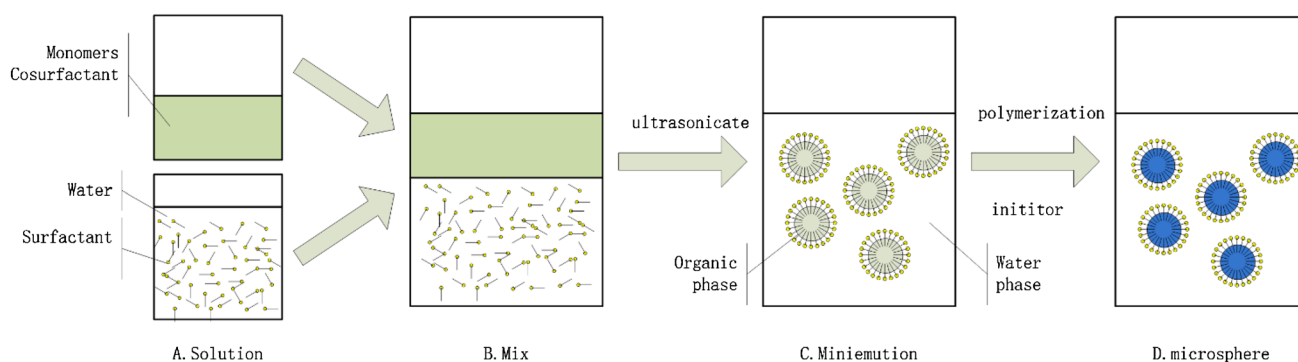
2.1 Materials

Styrene (St, > 98%), divinylbenzene (DVB, 95%, mixture of *m*- and *p*-isomers), vinyl benzyl chloride (VBC, 95%), and hexadecane (HD) were purchased from J&K Scientific Ltd (Beijing, China). *N*-propyl imidazole, sodium hydroxide (NaOH), potassium persulfate (K₂S₂O₈), polyvinyl pyrrolidone (PVP), ethyl cyanoacetate, methylbenzene, 2,2-azobisisobutyronitrile (AIBN), methanol and other chemicals (AR grade) were obtained from Beijing Chemical Works (Beijing, China). St and VBC were distilled under reduced pressure and stored in a freezer, AIBN was recrystallized, other chemicals were used as received.

2.2 Synthesis of PS-CH₂Cl Particles

2.2.1 PS-CH₂Cl Nanometer-Sized Particles (PS-CH₂Cl NPs)

The miniemulsion polymerization of cross-linked PS-CH₂Cl NPs (Scheme 1) was derived from a previous study of styrene polymerization [35], but the recipe has been changed based on a number of experiments. Firstly, a solution of 0.048 g of surfactant (SDBS) in 45 g of deionized water was prepared, in the meantime, 6 g of monomers mixture (volume ratio of VBC:DVB:St = 15:4:1) with 0.325 mL of HD were blended and stirred for 20 min. Then, two phases were mixed for 1 h at 300 r min⁻¹ for pre-emulsification. After that, the resultant mixture was sonicated for 10 min at 400 kW by using a Scientz-IID ultrasonic processor and turned into a white milk-like miniemulsion. The obtained miniemulsion was placed in a 250 mL four-necked flask, purged with the nitrogen for 30 min, and then heated to 70 °C. The polymerization was initiated by adding 0.12 g of KPS. The reaction usually continued for 4 h under a slow stirring. Finally, the product was filtered, washed repeatedly with ethanol and deionized water and dried under vacuum at 60 °C, and the white powder was obtained.



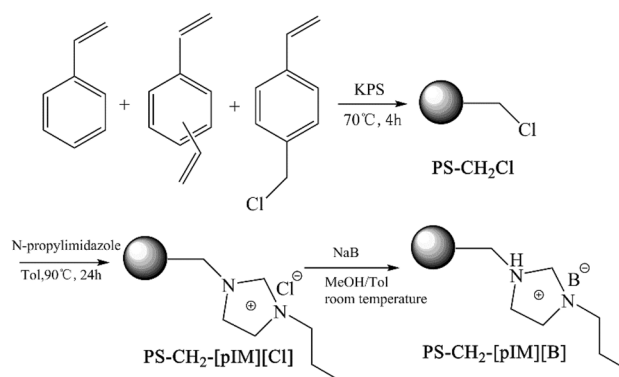
Scheme 1 The procedure of miniemulsion polymerization

2.2.2 PS-CH₂Cl Micrometer-Sized Particles (PS-CH₂Cl MPs)

In order to study the effect of the polymer particle size on the catalytic performance, PS-CH₂Cl MPs were synthesized by the polymerization of conventional free radical suspension according to the previous report as a comparison [36]. Firstly, 1.0 g of PVP, 3.0 g of sodium chloride were introduced into a round-bottomed flask containing 100 mL of deionized water, and stirred to become a transparent solution. Then, 6 mL of the monomer mixture (volume ratio of VBC:DVB:St = 15:4:1), and 0.5 g of AIBN were dissolved in 7.5 mL of toluene, introduced into a beaker and stirred to be homogeneous. Two solutions mentioned above were blended, the polymerization of conventional free radical suspension started at 75 °C and continued for 8 h under the protection of nitrogen atmosphere. Finally, the synthesized PS-CH₂Cl MPs were filtered and washed with hot water and methanol for three times to remove the dispersant PVP, the product was dried under vacuum at 50 °C for 8 h at last.

2.3 Synthesis of PS-CH₂-[pIM][B] Catalysts

The process for preparing PS-CH₂-[pIM][B] (B: basic anion) was shown in Scheme 2. Firstly, 1 g of PS-CH₂Cl particles were suspended in 40 mL of toluene and ultrasonicated for 1 h for well swelling. Secondly, *N*-propyl imidazole (triple molar equivalent of chloromethyl) was added into the suspension liquid, and the mixture was heated to 90 °C for 24 h. The product was washed with toluene, ethanol and methanol, successively, and dried under vacuum at 50 °C for 8 h. The resultant product was named as PS-CH₂-[pIM][Cl]. Finally, the PS-CH₂-[pIM][Cl] was dispersed in a sodium salt solution (NaOH, NaIm, or NaAc) with toluene-methanol mixed solvent with the volume ratio of toluene to methanol of 1:3, followed by stirring it at room temperature for 6 h. This process of ion exchange was repeated three times. After being washed with water and methanol, successively, and dried



Scheme 2 The procedure for preparing PS-CH₂-[pIM][B] catalyst

in a vacuum at 50 °C, the PS-CH₂-[pIM][B] catalyst was finally obtained.

2.4 Analytical Methods

Fourier transform infrared spectrometry (FTIR) analysis was conducted by using Shimadzu IR Affinity-1 s in a frequency range of 4000–450 cm⁻¹ with anhydrous KBr as dispersing agent. Thermogravimetric and differential thermal analysis (TG/DTA) was performed using WCT-1D by heating the samples under N₂ atmosphere with a heating rate of 10 °C min⁻¹ from room temperature up to 700 °C. Scanning electron microscopy (SEM) images were obtained with a JSM-7500F at 5 kV. The size distribution of particles was recorded on a Malvinic Mastersizer 2000. The specific surface values and pore volume were obtained from the BELSORP-max analyzer at 77 K. In addition, the alkali content of the prepared catalyst was determined by the titration method as follows. A certain volume of 0.020 mol L⁻¹ of benzoic acid in ethanol and 0.1 g of the catalyst were stirred at room temperature for 6 h and kept filtrate, then 0.01 mol L⁻¹ NaOH solution was used to titrate the filtrate containing the phenolphthalein indicator. When the color of

filtrate changed, the volume of the NaOH solution consumed was recorded and the alkali content of the catalyst was calculated in terms of the concentration of the known standard solutions and the mass of the catalyst.

2.5 Evaluation of Catalytic Performances

The catalytic performances of the catalysts prepared were evaluated by the Knoevenagel condensation of benzaldehyde with ethyl cyanoacetate. The amount of the catalyst was normally 0.2% of benzaldehyde molar amount in the reaction.

The Knoevenagel condensation of benzaldehyde with ethyl cyanoacetate is irreversible, as such, the catalytic performances of the catalysts were evaluated by using the conversion of benzaldehyde. The typical procedure was performed as follows. Reactants, benzaldehyde (10 mmol) and ethyl cyanoacetate (10 mmol) were poured into a 30 mL glass reactor containing 4 mL of solvent. The prepared catalyst was then added into this solution and the reaction was carried out at 60 °C. The agitation rate was kept at 300 rpm to ensure catalysts contact adequately with reactants. Samples were analyzed with high performance liquid chromatography (HPLC) equipped with an ultraviolet photometric detector (with a wavenumber of 254 nm). A Kromat C18 reversed phase silica gel column was used for test and the column temperature was maintained at room temperature. The mobile phase consisted of methanol and deionized water with a volumetric ratio of 9:1 at a flow rate of 0.3 mL min⁻¹.

In recycling experiments, catalysts were recovered by filtration through a 0.44 μm organic nano-filtration membrane, washed with ethyl acetate, ethanol and solvent, successively and then used in next time.

3 Results and Discussion

3.1 Characterization of Catalysts

FT-IR analysis was carried out to confirm the immobilization of basic ILs on cross-linked PS-CH₂Cl particles, as shown in Fig. 1. The characteristic peaks of benzene ring exhibited the C=C skeleton vibration at 1600, 1510 and 1450 cm⁻¹, the stretching vibration of C-H at 3024, 3057 and 3082 cm⁻¹, and the in-plane bending vibration of C-H at 1493 cm⁻¹. The absorption peak at 835 cm⁻¹ corresponds to the out-plane vibration of C-H bonds on the 1,4-disubstituted benzene ring, indicating the presence of para-disubstituted structural units in aromatic compounds in the sample. In addition, there are two strong absorption peaks at 2922 and 2850 cm⁻¹, which belong to the stretching vibration of C-H bonds in methylene groups, and the weaker absorption peak at 1361 represents its in-plane bending vibration [37]. These classical absorption peaks mentioned above were

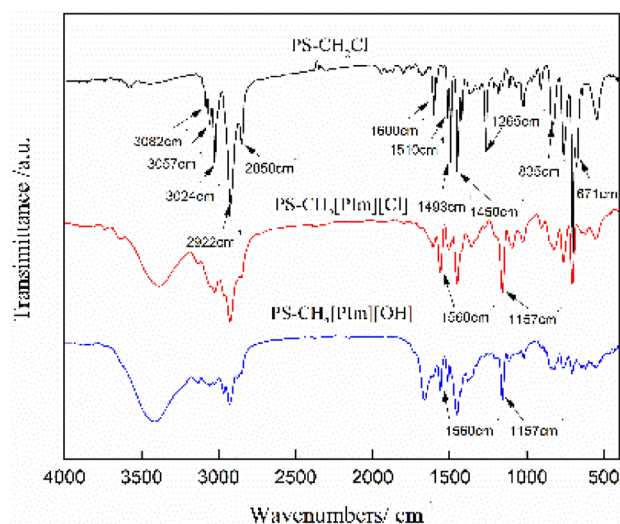


Fig. 1 FT-IR spectra of PS-CH₂-Cl, PS-CH₂-[pIM][Cl] and PS-CH₂-[pIM][OH]

observed from the absorption curves of all samples. From the infrared absorption spectrum of the PS-CH₂Cl sample, it can be seen that the stretching vibration absorption peak of C-Cl bonds at 671 cm⁻¹ and the in-plane bending vibration of C-H bonds in the methylene group linked to the chlorine atom at 1265 cm⁻¹, which indicated the presence of chloromethyl styrene structural units. However, they disappeared in the infrared absorption spectra of PS-CH₂-[pIM][Cl] and PS-CH₂-[pIM][B] samples, along with the appearance of absorption peaks at 1560 and 1157 cm⁻¹, which corresponding to the C=C and C=N vibrations of imidazole moiety, respectively. These proved that ILs were successfully loaded onto cross-linked polymer particles.

Independent and complete spherical morphology of catalysts were shown in Fig. 2. Nano-PS-CH₂-[pIM][B] presented a particle size distribution ranging from 50 to 300 nm and their average particle size of 137 nm, while they turned to be 50–300 and 147 μm respectively for the micro-PS-CH₂-[pIM][B] (Fig. 2d). The miniemulsion polymerization used in here is advantageous in a high polymerization rate due to no existence of monomer diffusion phenomenon. The particle size of the prepared particles mainly depends on the size of the monomer droplets, and generally distributes between 50 and 500 nm [38, 39]. It explains the narrow particle size distribution for the prepared particles. The particle size distribution of the PS-CH₂Cl particles prepared in this work was relatively larger mainly due to the high content of DVB. It has been proved by previous report [40] that the increasing amount of the crosslinking agent led to a wider size distribution. In comparison with PS-CH₂-Cl particles, the introduction of ILs onto polymer particles made their surface smoother. In comparison with fresh PS-CH₂-[pIM][OH] (Fig. 2b, c), the morphology of

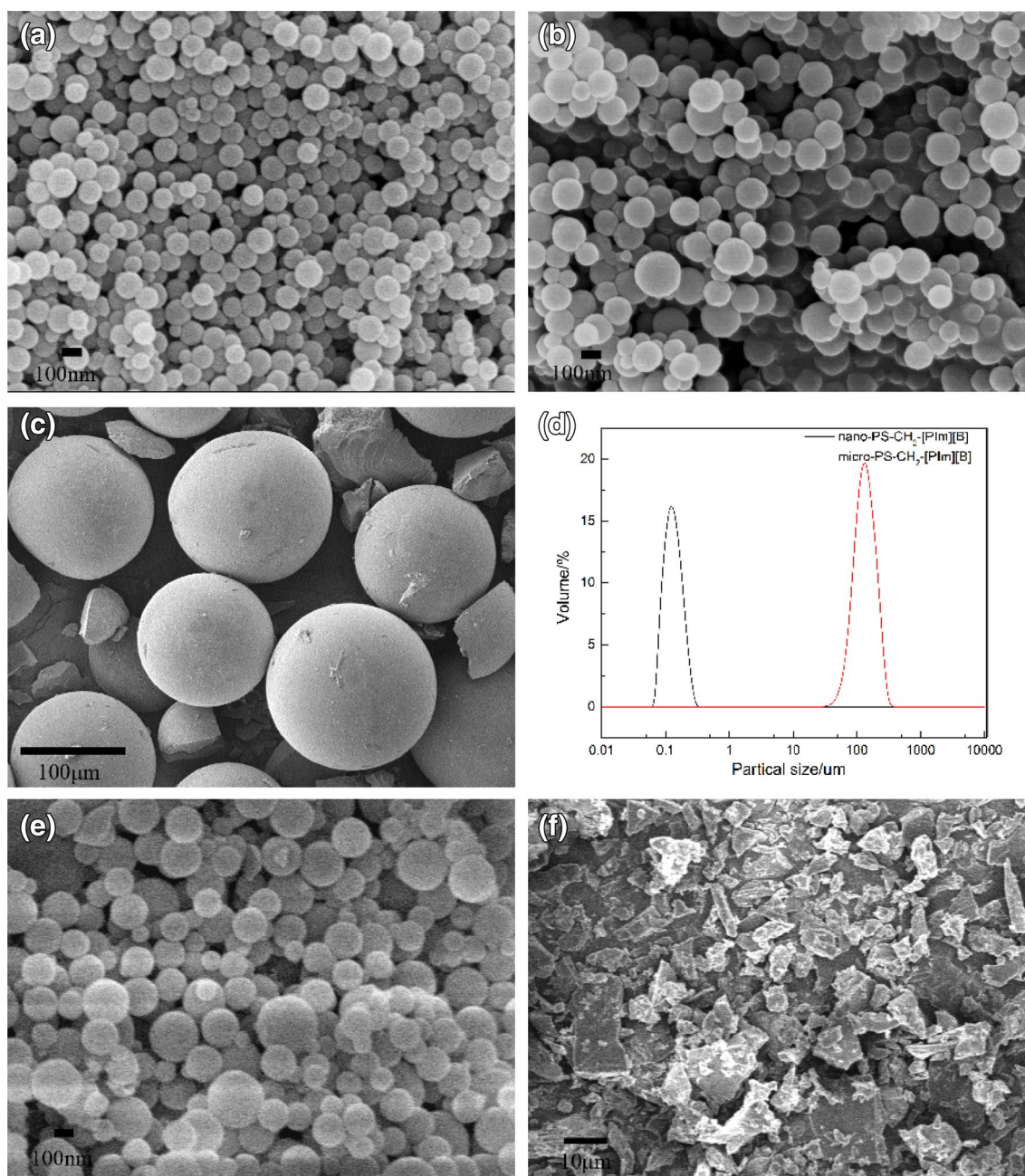


Fig. 2 SEM images of PS-CH₂-Cl NPs (a), nano-PS-CH₂-[pIM][OH] (b) and micro-PS-CH₂-[pIM][OH] (c), and size distribution of PS-CH₂-[pIM][B] particles (d), nano-PS-CH₂-[pIM][OH] (e) and micro-nano-PS-CH₂-[pIM][OH] (f) reused for eight times

reused nano-PS-CH₂-[pIM][OH] (Fig. 2e) had no obvious change, which attributed to its high cross-linked structure. However, micro-PS-CH₂-[pIM][OH] (Fig. 2f) was destroyed after recycling even same amount cross-linked agent was used, which affected its catalytic performance to a little bit improvement in second reuse.

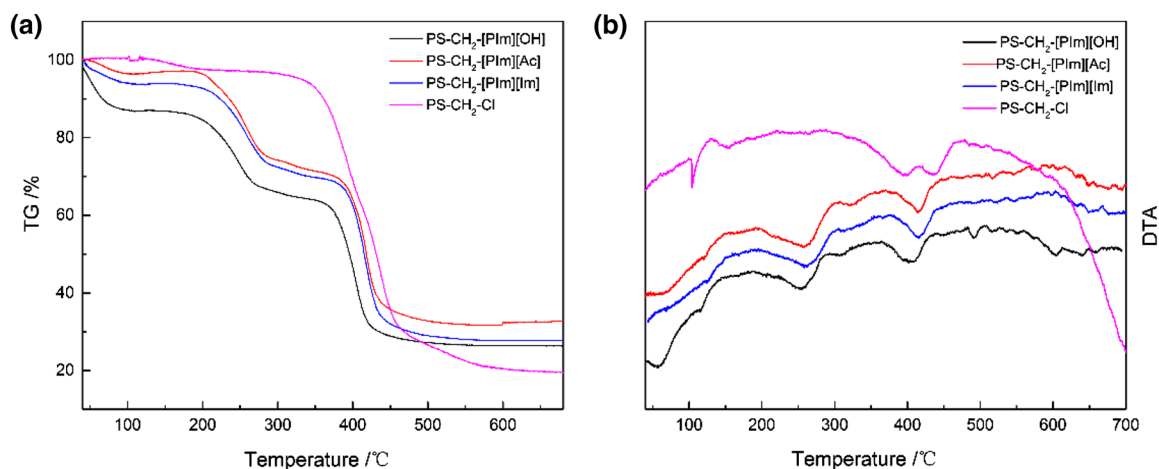
EDS reflected the relative elements contents (N, Cl) on the surface of PILs as shown in Table 1. Three places were selected for the measurement. The relative elements contents

of Cl were lower than theoretical value, which indicated that the actual monomer ratio in the polymer was little different from monomer feed ratio. ILS section distributed on the surface of PS from the increasing element content of N, it demonstrated that ILS were immobilized on cross-linked polymer particles and ILS loading ratio is over 85%.

TG-DTA analysis was carried out to investigate the thermal stability of PS-CH₂-Cl and PS-CH₂[pIM][B] catalysts, as shown in Fig. 3. The weight loss was both observed

Table 1 Element amount of PS-CH₂Cl and PS-CH₂-[pIM][Cl]

	PS-CH ₂ Cl			PS-CH ₂ -[pIM][Cl]		
	V _{Theo}	Nano	Micro	V _{Theo}	Nano	Micro
Cl (atom%)	7.19	5.19	5.09	0	0	0
N (atom%)	4.56	3.73	3.56	9.13	7.92	7.50
ILs loading amount (mmol g ⁻¹)	–	–	–	4.91	4.27	4.04

**Fig. 3** TG-DTA patterns of PS-CH₂-Cl and PS-CH₂-[pIM][OH]

from PS-CH₂-Cl and PS-CH₂[pIM][B] below 200 °C, it is attributed to the physically adsorbed solvent, and the hydrophilic structure of ILs facilitated PS-CH₂[pIM][B] absorption of more solvent. The introduction of ILs led the temperature of initial weight loss of the product rising up to nearly 270 °C. The weight loss at this temperature is due to the breakage of the bonds of imidazolium to the carrier. When the temperature further increased up to higher than 350 °C, the weight loss was clearly observed in the curves of both PS-CH₂Cl and PS-CH₂[pIM][B] which correspond to the fracture and cracking of main polymer chains. Until around 600 °C, there was no longer weight loss, remaining nothing but residual carbon. Therefore, it suggested that the catalyst can be used under 200 °C. There were no obvious differences among PS-CH₂[pIM][B] catalysts, but a tiny disparity of second peak of DTA curve in Fig. 3b. It showed that PS-CH₂-[pIM][OH] lost weight at the lowest temperature, while PS-CH₂-[pIM][Ac] lost weight at the highest temperature. It possibly owned to the interaction between the anion and carrier.

BET reflected the pore structure of PS-CH₂Cl as shown in Table 2, nano-PS-CH₂Cl with a specific surface area more than 20 m² g⁻¹ and 2.59 nm of pore diameter which can be considered as the channel of nanoparticles accumulation rather than the pores of the particles themselves. The specific surface area of micro-PS-CH₂Cl is too small to measure.

Table 2 BET characterization data for PS-CH₂Cl

Sample	BET SA (m ² g ⁻¹)	BJH V _p (cm ³ g ⁻¹)	BJH D _p (nm)
Nano-PS-CH ₂ Cl	21.72	0.092	2.59
Micro-PS-CH ₂ Cl	< 1	–	–

Table 3 Akali amount of PS-CH₂-[pIM][B]

Catalysts	Alkali amount (mmol g ⁻¹)
Nano-PS-CH ₂ -[pIM][OH]	1.1012
Nano-PS-CH ₂ -[pIM][Ac]	1.2010
Nano-PS-CH ₂ -[pIM][Im]	1.2133
Micro-PS-CH ₂ -[pIM][OH]	0.6811

The alkali amount of the PS-CH₂-[pIM][B] was carried out by the titration method and results were shown in Table 3. Overall, nano-PS-CH₂-[pIM][B] have a higher alkali amount, more than 1 mmol g⁻¹. It is known that the polymer carriers are porous [36], and there exists a diffusion process of basic anions during the ion exchange step. The smaller the diffusion resistance is, the more conducive to ion exchange is. Compared to micrometer-sized carrier,

nanometer-sized carrier has a higher specific surface area, and its diffusion resistance is greatly reduced or even negligible for its pores, so that more bases were supported. Notably, the basic ion exchange is an important step in the preparation process; moreover, multiplying the ion exchange process plays a more significant role than extending time.

3.2 Catalytic Performances of PS-CH₂-[pIM][B] Catalysts

To evaluate the PS-CH₂-[pIM][B] described here, the catalytic activities for Knoevenagel condensation were examined under the same reaction conditions as shown in Table 4. Obviously, the carrier PS-CH₂-Cl showed almost no catalytic activity, because the yield was nearly similar to the sample without catalyst. In addition, PS-CH₂-[pIM][Cl] showed a weak catalytic activity for the weak Lewis basic strength of Cl⁻, while PS-CH₂-[pIM][B] showed a better catalytic activity. It means that the reaction was mainly catalyzed by the loaded basic anions. The catalytic activity of catalysts with different alkali anions was various. It was obvious that nano-PS-CH₂-[pIM][OH] had a higher catalytic efficiency with 94% of yield, as well as the homogeneous catalyst NaOH. The catalytic activity of nano-PS-CH₂-[pIM][Ac] was relatively lower, which is related to the base strength. However, Im⁻ showed a bit lower catalytic efficiency than OH⁻, although its base strength is theoretically stronger than that of OH⁻. It is probably due to the volume of Im⁻, which is too large to hinder the diffusion of reactants. The catalytic efficiency of micro-PS-CH₂-[pIM][OH] was no better than that of nano-PS-CH₂-[pIM][OH], because of its greater diffusion resistance. Additionally, it was found that a higher catalyst loading corresponds to a higher catalytic efficiency (Samples 4–7 in Table 4), and increasing catalytic active

sites is conducive to the conversion of reactants. However, the conversion tends to a balance, when the catalyst amount exceeds a certain limit. Overall, these catalysts were efficient in this reaction system.

Meanwhile, the reusability of PS-CH₂-[pIM][B] catalysts was evaluated by catalyzing Knoevenagel condensation in methanol (Fig. 4a) and aqueous phase (Fig. 4b), respectively. Catalysts were recovered by filtration through a 0.44 μm organic nano-filtration membrane. It's obvious that micro-PILs is recovered quickly than nano-PILs, but both of them could be recovered with negligible loss, which was reflected by yield in recycling experiment. In methanol phase, the catalytic performance of micro-PS-CH₂-[pIM][OH] improved in the second time, which mainly because it cracked into smaller particles and decreased diffusion resistance. Eventually, its catalytic activity decreased 4.13%. Comparatively, that of the nano-PS-CH₂-[pIM][OH] decreased 9.36%. Even so, the loss in catalytic activity reached 5.47% for nano-PS-CH₂-[pIM][Im] and 4.83% for nano-PS-CH₂-[pIM][Ac] which exhibited an excellent stability and reusability of nano-PS-CH₂-[pIM][B].

Reactants and products are easily soluble in methanol and the catalyst disperses well in methanol, so that they well contacted with each other during the whole reaction process, and the reaction achieved a relatively high yield. However, the situation changes greatly when the solvent was replaced by water. Firstly, the reactants are hardly soluble in aqueous phase, which results in insufficient contact between the reactants and the catalyst. Secondly, water as one of the products in the condensation inhibits the forward course of the reaction, hence, the yield turns out to be very low, nearly 30% without catalyst.

Surprisingly, the prepared nanometer-sized alkaline catalysts exhibited an efficient catalytic performance for the

Table 4 Activities of various catalysts for Knoevenagel condensation

Samples	Catalysts	Catalyst loadings (%) ^a	Yeild (%)	Selectivity (%)
1	Blank	0	75.25	100
2	Nano-PS-CH ₂ -Cl	— ^b	74.98	100
3	Nano-PS-CH ₂ -[pIM][Cl]	— ^b	77.01	100
4	Nano-PS-CH ₂ -[pIM][OH]	0.1	86.88	100
5	Nano-PS-CH ₂ -[pIM][OH]	0.2	93.99	100
6	Nano-PS-CH ₂ -[pIM][OH]	0.4	94.58	100
7	Nano-PS-CH ₂ -[pIM][OH]	0.6	94.95	100
8	Nano-PS-CH ₂ -[pIM][Ac]	0.2	84.12	100
9	Nano-PS-CH ₂ -[pIM][Im]	0.2	89.62	100
10	Micro-PS-CH ₂ -[pIM][OH]	0.2	88.19	100
11	NaOH	0.2	92.73	100

Reaction conditions: n_{benzaldehyde} = n_{ethyl cyanoacetate} = 0.1 mol, 4 mL of methanol as solvent, 60 °C, 4 h

^an_{alkali}:n_{benzaldehyde}

^bThe same weight as catalyst of sample 5

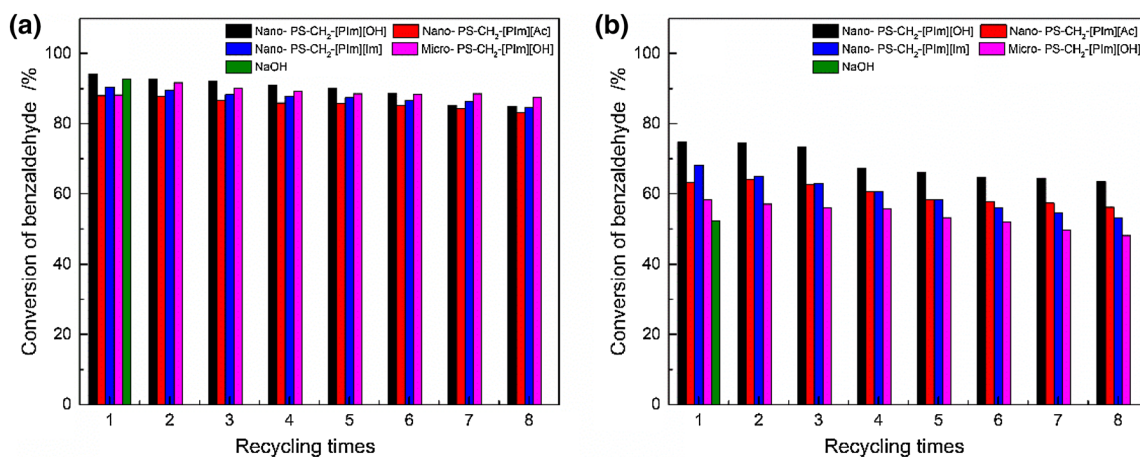


Fig. 4 Recycling of PS-CH₂-[pIM][B] for Knoevenagel condensation in methanol (a) and aqueous phase (b)

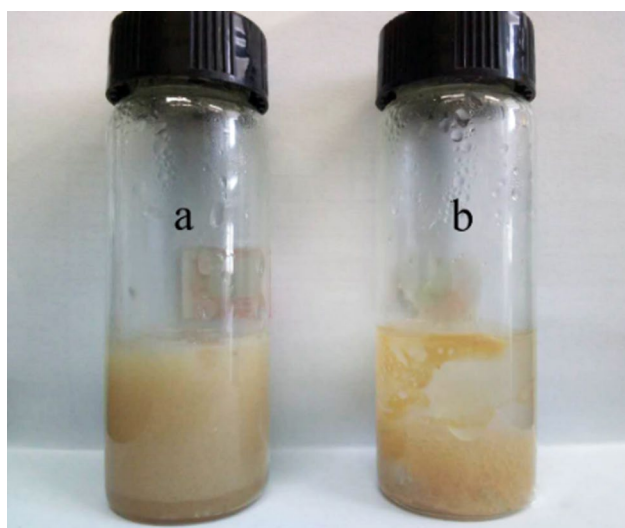
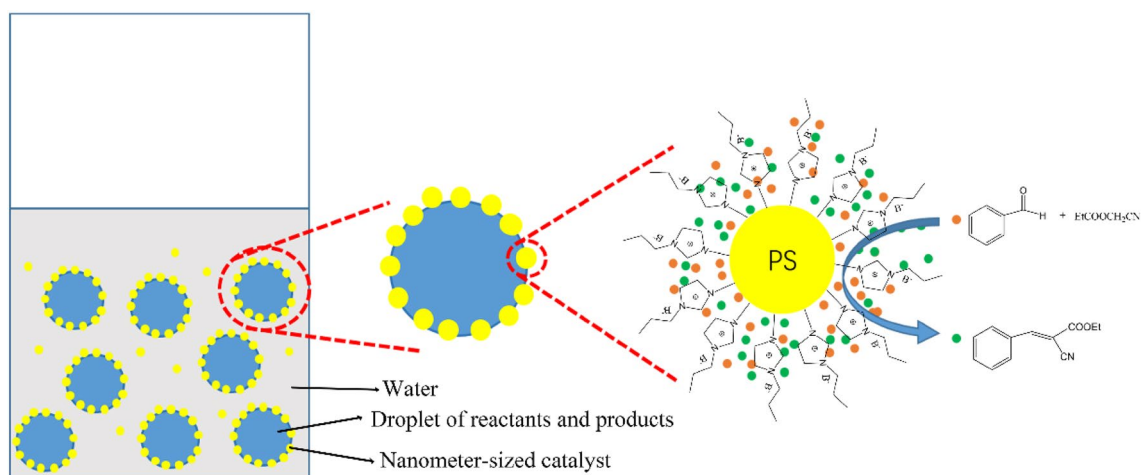


Fig. 5 Dispersion of nano-PS-CH₂-[pIM][OH] (a) and micro-PS-CH₂-[pIM][OH] (b) for Knoevenagel condensation in aqueous phase

Knoevenagel condensation in aqueous phase. As shown in Fig. 4b, nano-PS-CH₂-[pIM][B] provided more excellent catalytic activities. Especially for nano-PS-CH₂-[pIM][OH], its yield even reached 74%, and kept over 63% after reusing 8 times, which was much higher than that for NaOH and micro-PS-CH₂-[pIM][OH]. Nano-PS-CH₂-[pIM][Ac] showed a relatively lower but still more stable catalytic efficiency, nevertheless, its catalytic efficiency reduced more in aqueous than in methanol. It may be due to the more ions exchanging in water so that the more active ions lose, or, the insoluble product covered the surface of the catalyst as a solid, which led to the decrease of catalytic efficiency.

As shown in Fig. 5a, the prepared nano-PS-CH₂-[pIM][OH] evenly dispersed in the system with water as a solvent. Based on the results above, a catalytic mechanism for Knoevenagel condensation over the prepared nano-PS-CH₂-[pIM][B] in aqueous phase is proposed in Scheme 3. The small catalyst particles played a role of a surfactant, and presented in the oil–water interface, which allowed more



Scheme 3 Catalytic mechanism of nano-PS-CH₂-[pIM][OH] for Knoevenagel condensation

uniform and sufficient contact with substances. Furthermore, they can be regarded as solid extractants, because of the enrichment of active sites. Reactants tend to enrich on their surfaces and convert, and then be catalyzed greatly. Based on this explanation, the smaller the catalyst particles were, the better the catalytic performance was. It also explains why nano-PS-CH₂-[pIM][B] were more efficient than micro-PS-CH₂-[pIM][B] in aqueous phase.

In order to further explore the catalytic performance of the prepared nano-PS-CH₂-[pIM][OH] for the condensation reaction, the experimental group of nano-PS-CH₂-[pIM][OH] catalyzed Knoevenagel condensation in different solvents were carried out (Table 5). It was found that the greater the polarity of the solvent was, the higher the yield was. mainly because polar solvents benefit ILs, the polar parts of catalysts, fully stretching to contact with reactants, and facilitates the transformation of the reactant structure. Unfortunately, any important relationship between the swelling of the polystyrene particles [41] and its catalytic performance in Knoevenagel condensation has not be found yet.

4 Conclusions

Polystyrene nanometer-sized particles supported basic imidazolium ionic liquids were synthesized and their performances were evaluated by the Knoevenagel condensation of benzaldehyde with ethyl cyanoacetate. The cross-linked PS-CH₂Cl NPs with narrow particle size distribution were prepared by miniemulsion polymerization, the ionic liquids were successfully loaded on these carriers by covalent bond, and their alkali amounts were more than 1 mmol g⁻¹. The prepared nano-PS-CH₂-[pIM][B] catalysts exhibited a good thermal stability and an excellent catalytic activity for Knoevenagel condensation both in methanol and aqueous phase. Notably, the yield for nano-PS-CH₂-[pIM][OH] catalyzing Knoevenagel condensation in aqueous phase reached 74%, and kept over 63% after eight times reusing. Compared

to micro-PS-CH₂-[pIM][B] prepared by the suspension polymerization, the nanometer-sized catalysts performed charming reusability and stability due to the advantages of their nanometer size. We believe that nano-PS-CH₂-[pIM][B] catalyst will have a significant potential application for organic reaction in aqueous phase.

Acknowledgements We are very grateful to the National Natural Science Foundation of China (NNSFC) for the support (No. 21576025).

Compliance with Ethical Standards

Conflict of interest The authors declare that they have no conflict of interest.

References

1. Wilkes JS (2004) *J Mol Catal A* 214:11
2. Ni B, Headley AD (2010) *Chemistry* 16:4426
3. Lee JW, Shin JY, Chun YS (2010) *Acc Chem Res* 43:985
4. Qiao K, Deng Y (2001) *J Mol Catal A* 171:81
5. Mehnert CP, Mozeleski EJ, Cook RA (2003) *Chem Commun* 34:3010
6. Riisager A, Jørgensen B, Wasserscheid P (2006) *Chem Commun* 37:994
7. Liu S, Lu LI, Shitao YU (2010) *Chin J Catal* 31:1433
8. Durand J, Teuma E, Gómez M (2007) *Cr Chim* 10:152
9. Mehnert CP, Cook RA, Dispenziere NC (2002) *J Am Chem Soc* 124:12932
10. Zhu A, Jiang T, Han B, Zhang J, Xie Y, Ma X (2007) *Green Chem* 38:169
11. Shao Y, Wan H, Miao J, Guan G (2013) *React Kinet Mech Cat* 109:149
12. Wu X, Wang M, Xie Y, Chen C, Li K (2016) *Appl Catal A* 519:146
13. Lin Y, Wang F, Zhang Z, Yang J, Wei Y (2014) *Fuel* 116:273
14. Movahed SK, Esmatpoursalmani R, Bazgir A (2014) *RSC Adv* 4:14586
15. Rodríguezpérez L, Teuma E, Falqui A, Gómez M, Serp P (2008) *Chem Commun* 35:4201
16. Yuan H, Jiao QZ, Zhang Y, Zhang J, Wu Q (2016) *Catal Lett* 146:1
17. Dr CPM (2004) *Chem Eur J* 11:50
18. Zhang Q, Zhang S, Deng Y (2011) *Green Chem* 13:2619
19. Patra T, Karmakar S, Upadhyayula S (2017) *Tetrahedron Lett* 58:1531
20. Valkenberg MH, Decastro C, Hölderich WF (2001) *Top Catal* 14:139
21. Qiu XH, Xie Y, Wang XY et al (2013) *Asian J Chem* 25:1673
22. Kumar P, Vermeiren W, Dath JP, Hoelderich WF (2006) *Appl Catal A* 304:131
23. Wang G, Yu N, Lin P et al (2008) *Catal Lett* 123:252
24. Dötterl M, Helmut G (2012) *Chemcatchem* 4:660
25. Kim JH, Kim JW, Shokouhimehr A, Lee YS (2005) *J Org Chem* 70:6714
26. Karbass N, Sans V, Garcia-Verdugo E, Burguete MI, Luis SV (2006) *Chem Commun* (29):3095
27. Itoh H, Naka K, Chujo Y (2004) *J Am Chem Soc* 126:3026
28. Huang J, Jiang T, Gao H, Han B, Liu Z, Wu W, Chang Y, Zhao G (2004) *Angew Chem Int Ed* 43:1397

Table 5 Nano-PS-CH₂-[pIM][OH] for Knoevenagel condensation in different solvents

Samples	Solvent	Yeild (%)	Selectivity (%)
1	DMSO	96.42	100
2	DMF	93.95	100
3	Methanol	93.99	100
4	Ethanol	92.15	100
5	Water	74.73	100
6	Tetrahydrofuran	74.88	100
7	Methylbenzene	46.14	100
8	Cyclohexane	33.14	100
9	No solvent	66.67	100

29. Kume Y, Qiao K, Tomida D, Yokoyama C (2008) *Catal Commun* 9:369
30. He X, Liu Z, Fan F, Qiang S, Cheng L, Yang W (2015) *J Nanopart Res* 17:1
31. Wang T, Wang W, Yuan L, Chen X, Li C, Zhang Y (2017) *RSC Adv* 7:2836
32. Burguete MI, Erythropel H, Garcia-Verdugo E, Luis SV, Sans V (2008) *Green Chem* 10:401
33. Sugimura R, Qiao K, Tomida D, Yokoyama C (2007) *Catal Commun* 8:770
34. Xu Z, Wan H, Miao J, Han M, Yang C, Guan G (2010) *J Mol Catal A* 332:152
35. Landfester K, Bechthold N, Franca Tiarks A, Antonietti M (1999) *Macromolecules* 32:5222
36. Liu QQ, Li W, Yu HJ, Tan QH (2008) *Eur Polym J* 44:2516
37. Quiñones R, Gawalt ES (2008) *Langmuir* 24:10858
38. Schork FJ, Luo Y, Smulders W, Russum JP, Butté A, Fontenot K (2005) *Adv Polym Sci* 175:129
39. Baruch-Sharon S, Margel S (2010) *Colloid Polym Sci* 288:869
40. Shlomo M, Eliahu N, Inna F (1991) *J Polym Sci Pol Chem* 29:347
41. Davankov VA, Pastukhov AV, Tsyurupa M (2000) *Polym Sci* 38:1553

Affiliations

Min Ma¹ · Hansheng Li¹  · Wang Yang¹ · Qin Wu¹ · Daxin Shi¹ · Yun Zhao¹ · Caihong Feng¹ · Qingze Jiao^{1,2}

¹ School of Chemistry and Chemical Engineering, Beijing Institute of Technology, Beijing 100081, China

² School of Chemical Engineering and Materials Science, Beijing Institute of Technology, Zhuhai, Zhuhai 519085, China